



12<sup>th</sup> International Conference on  
Multimedia in Physics Teaching and Learning,  
13-15 September 2007, Wrocław, Poland

*Conference Proceedings*

**Wiesław Tłaczała<sup>1</sup>, Marek Szymański<sup>1</sup>, Gabriel Gorghiu<sup>2</sup>, Alfred Zagórski<sup>1</sup>, Marcin Zaremba<sup>1</sup>**

<sup>1</sup> **Warsaw University of Technology, Warsaw, Poland**

<sup>2</sup> **Valahia University Targoviste, Targoviste, Romania**

***Virtual Physics Laboratory – Selected Topics***

In the paper we present the set of eight experiments developed for the VccSSe (*Virtual Community Collaborating Space for Science Education*) project and devoted to heat conductivity, Curie temperature determination, electrical resonance, gamma rays absorption, horizontal component of the geomagnetic field determination, and gas laws. The presented set of the simulated physics experiments are included in a specific module for training, dedicated for the in-service teachers training, in the frame of a recent approved European Socrates project: 128989-CP-1-2006-1-RO-COMENIUS-C21. The presented experiments can be also useful for students for the training before entering the real physics laboratory.

*Introduction*

Physics experiment is unquestionably necessary for physics teaching and is a part of study programs of physicists and specialists in many fields, from engineering to health care. However, the experiments necessary for teaching are not available everywhere, mainly due to financial or organizational constraints. Because of this, simulated experiments are proposed as an educational tool to substitute real experiments in places where they cannot be performed. Simulated experiment is an experiment where standard multimedia computer with appropriate software simulates chosen physical phenomena. Simulated experiments can be helpful when real experiments are unavailable, for example in schools or at home. They can be used by teachers and lecturers for demonstrational purposes or by school and university students during learning. Simulated experiments are especially useful for distant learning, disabled students and for preparation for classes in real laboratory. Additionally they are completely safe and may introduce physics to young people with special interests in computers.

*Approach*

There are two ways of understanding the term “simulated experiment”:

- an application demonstrating pure physical phenomena, focusing on mathematical model describing it;
- an application attempting to reproduce real experiment as exactly as possible, focusing not only on the underlying physical phenomena, but also on how it is observed and measured.

Our simulated experiments are realized according to the second definition. It means that we attempt to create interactive applications showing real experiments performed by students, with special emphasis on measurement method, used instruments and experiment performing. The real and virtual versions of the experiments are as similar as possible and they have the same goals, the same instruments are used and the same physical quantities are measured. To perform the simulated experiment, user must perform the same steps as in real laboratory:

read experiment instruction (the same for real and virtual version), complete and prepare experimental setup, perform measurement and in the end, analyze data obtained in the experiment on his own in a general purpose application, i.e. Excel, to get the final result and its uncertainty. It is worth noting that our experiments can go wrong. If the user makes a mistake, he can measure wrong physical quantities or even measure nothing at all if there is a problem with experimental setup. In that case, it will be impossible to determinate the final outcome of experiment.

From the technical point of view, our experiments are applications created in LabVIEW environment. LabVIEW has important advantages that make it a very useful tool for development of interactive applications such as simulated experiments. The primary advantages are: exceptional ease of creating working, reliable applications and the supplied library of graphical controls and indicators imitating parts of real instruments, such as knobs, switches and displays. For us, yet another advantage of LabVIEW was the possibility of reusing graphical user interfaces of before developed applications controlling real experiments so that virtual and real versions look the same.

For end user to begin the simulated experiment, he has to run our application from any media (i.e. CD-ROM) or from the Internet, if the experiment was published on a webpage. It is important that the end user does not have to pay any license fees related to the fact that the experiments were developed in LabVIEW, because only application developer has to pay for LabVIEW license. Our virtual experiments are prepared for Windows, but can be run under any operating system with LabVIEW Run-Time Engine installed, which can be downloaded for free from National Instruments website.

### *Experiments*

In the work we present a set of the following experiments: tangent galvanometer, laws of gases, gamma absorption studies, Curie temperature determination for ferromagnetic materials, heat transportation studies, electrical resonance studies. In the following subsections the experiments will be briefly described and their most important features will be mentioned.

#### **Tangent galvanometer**

Tangent galvanometer is a classic experiment, where the horizontal component of geomagnetic field is measured using a coil and a magnetic needle. In the experiment the magnetic field rotating needle is a superposition of horizontal component of geomagnetic field, which is unknown, and magnetic field generated by coil, which is assumed to be known. By measuring the needle rotation angle in function of coil current, with known coil geometry and number of loops, it is possible to calculate the value of horizontal component of earth magnetic field.

To perform the experiment, the user should read the experiment description and instructions and run our application. The first step is preparation of virtual experimental setup. The relevant window is seen below (Fig. 1).

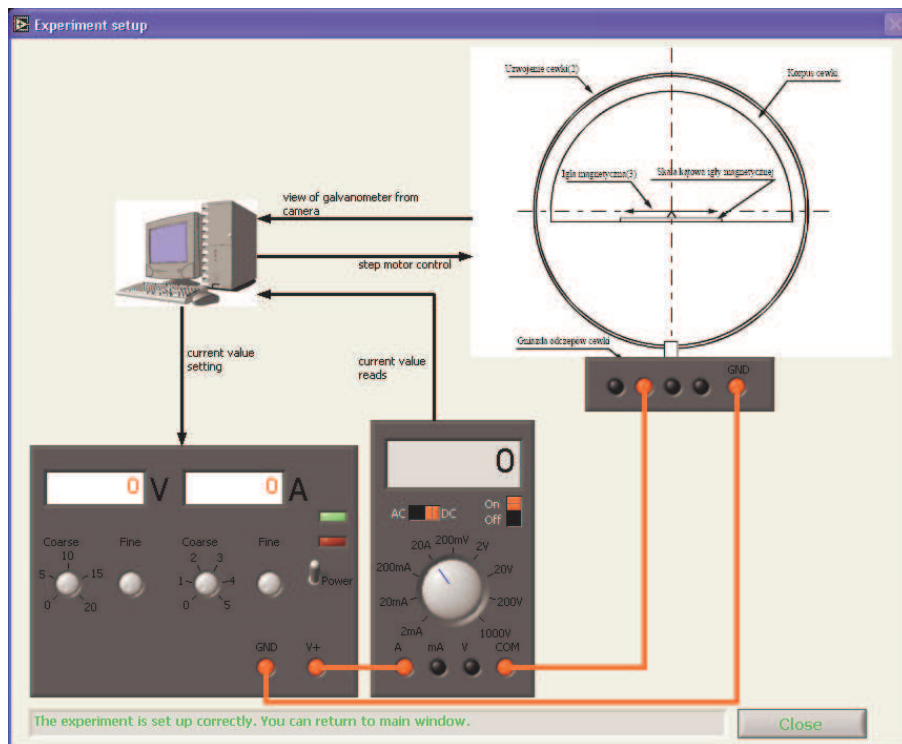


Fig. 1

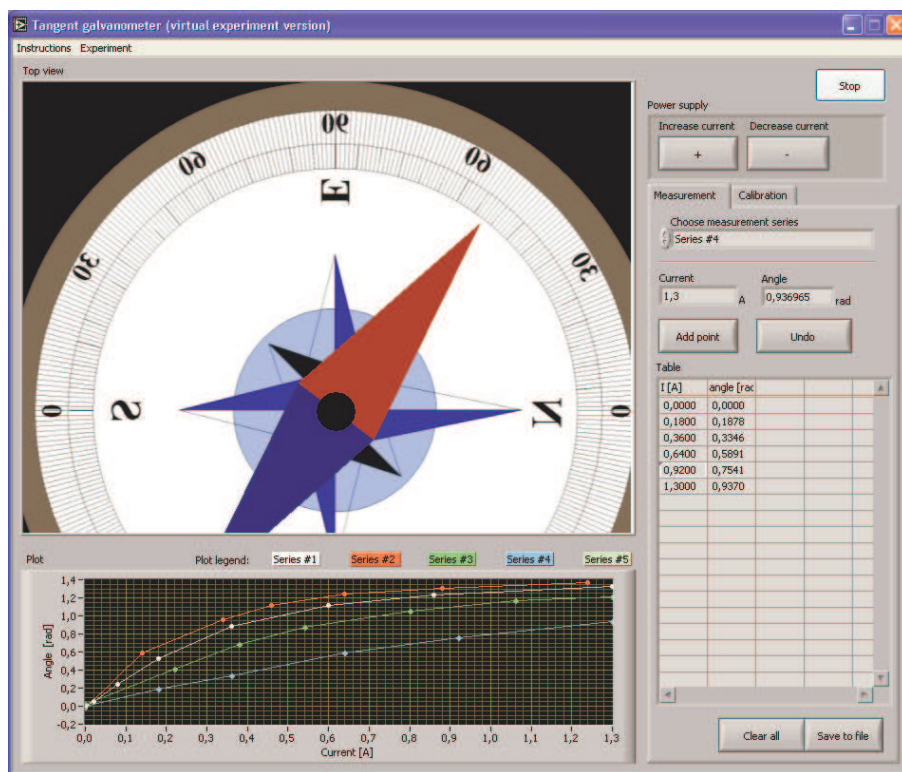


Fig. 2

In the window there are power supply, multimeter and coil. Preparation of experimental setup consists of connecting the visible instruments with cables, setting up the instruments with

switches and knobs and turning them on. It is worth noting, that many different connection configurations are possible and they correspond to different number of loops in the coil. At the bottom of the window there is a message indicating if the experiment is set up correctly. If the experiment configuration is invalid or may cause instrument damage it is impossible to turn on the current and perform any measurements.

After setting up the experiment, it is possible to start measurement as can be seen in Fig 2. The angle measurement is realized by clicking on the red end of the magnetic needle. The program presents the results gathered in the form of table and on the plot, on which results obtained for different number of loops in coil are shown all together. After completing the measurement it is possible to save data gathered to a text file. After data saving, the experimental part is completed and our application can be closed.

To complete the experiment, the student has to analyze the results on his own to calculate the value of horizontal component of geomagnetic field and its uncertainty. This can be done in many ways, and it's up to student to choose the method and perform the calculations in general purpose applications, such as Excel or Matlab.

### **Gamma absorption studies**

In this experiment gamma ray absorption is demonstrated (Fig. 3). It is shown that the intensity decreases exponentially with the thickness of absorber, and effectiveness of different absorbers, such as lead and cooper, are compared.

The total absorption coefficient of  $\gamma$ -rays represents, in fact, the intensity attenuation of the photon beam when it passes through the matter. The  $\gamma$ -rays intensity  $I(x)$  decreases exponentially with respect to the thickness of the absorber as following:

$$I(x) = I_0 \exp(-\mu x), \quad (1)$$

where:  $I_0$  - entire beam intensity;  $x$  - thickness of the absorber;  $\mu$  - total absorption coefficient.

Preparation of the experiment requires placing gamma source in the measurement system and setting up the detector. The detector is powered by high voltage power supply and in the simulated experiment we use this opportunity to teach the students a safe practice of not turning on the power supply if the voltage set is not zero. As a result of the experiment, exponential curves of decrease of gamma ray intensity are obtained for different materials, and after finishing the experimental part students should calculate attenuation coefficients for the samples used.

The user can perform experiment with  $^{137}\text{Cs}$  and  $^{60}\text{Co}$  sources and examine the  $\gamma$  -ray absorption law (1) for samples made of lead and cooper. After acquiring, data are plotted on the graphs (Fig. 3) commonly with the curves obtained using exponential fitting.

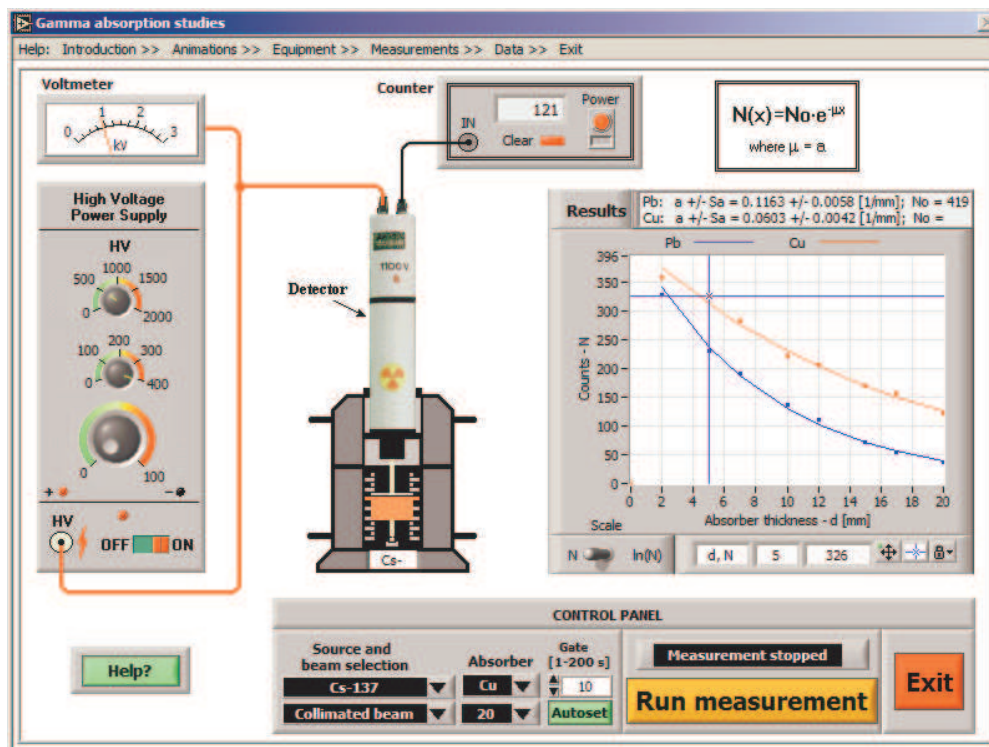


Fig. 3

## Curie temperature determination for ferromagnetic materials

The virtual experiment, which demonstrates phase transition, on an example of measurement Curie temperature for ferromagnetic materials, is shown in Fig. 4.

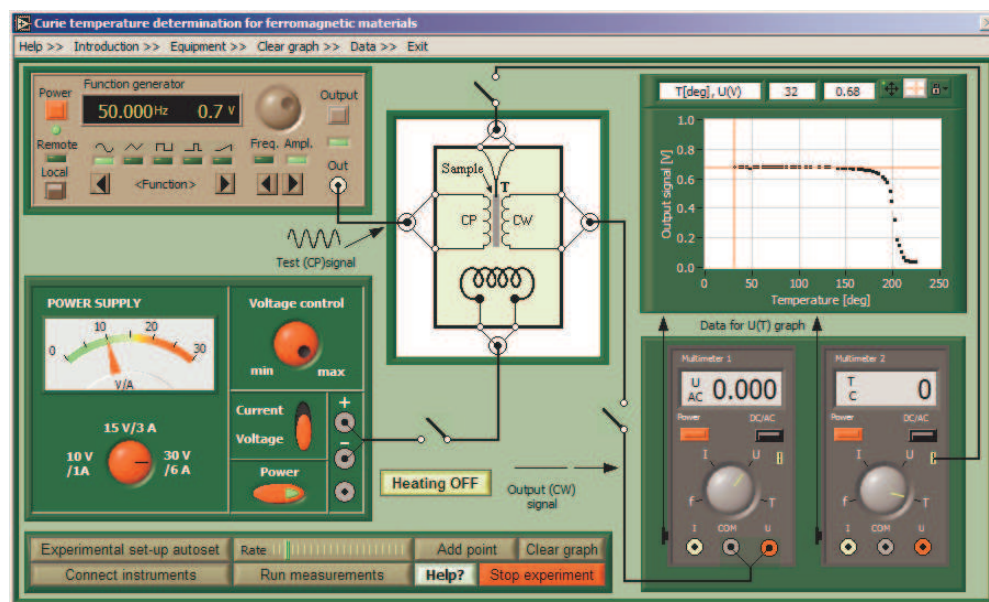


Fig. 4



As it is well known, ferromagnetic materials (usually alloys based on iron) lose their magnetism above certain temperature called the Curie temperature  $T_c$ . For iron it is 770 °C. The typical plot of magnetisation ( $M$ ) as function of the temperature is shown in Fig. 5.

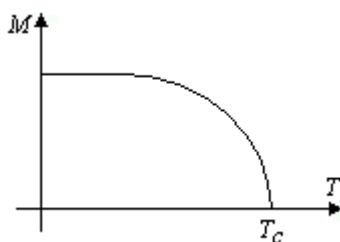


Fig. 5

Below  $T_c$  ferromagnetic materials exhibit spontaneous magnetisation – its elementary magnets (spins) interact with each other in such a way, that they order their directions. Above this temperature thermal fluctuations of spins are so large that material loses its ordering and becomes paramagnetic.

The transition from the ferromagnetic to paramagnetic phase can be observed in a transformer with an iron core. The voltage induced in the secondary coil depends essentially on the value of magnetic permeability of the core. When heating the temperature of the core increases and finally reaches  $T_c$ . In this moment the voltage on secondary coil decreases rapidly and may be observed on a multimeter display. After finishing the measurements, the students have to determine Curie temperature for his sample.

### Heat transportation studies

In this case one measures the thermal conductivity coefficient  $\lambda$  for a metallic rod. It has the meaning of the quantity of heat  $\Delta Q$  transferred through the material in unit time  $\Delta t$ , with the cross-section  $S$  and unit gradient of the temperature  $\text{grad } T$  (Fig. 6a). In mathematical formulation

$$\Delta Q = \lambda S (\text{grad } T) \Delta t. \quad (2)$$

The value of the thermal conductivity coefficient is different for different materials and characterises, for instance, the isolation characteristics of materials. For iron  $\lambda = 79$  [SI units], for water  $\lambda = 0.6$  etc.

Presented experiment is based on the Ångström method. It demonstrates the damping of temperature variations in a rod. The temperature changes are generated by repeatedly switching on/off the heating system installed on the one end of the rod. This produces a temperature “wave” which penetrates the rod. These changes propagate through the whole sample but with the amplitude decreasing (exponentially) with increasing distance  $x$  from the source of heat. The temperature  $T$  is then described by a function typical for all damped waves:

$$T(x, t) = (T_0 e^{-ax}) \cos[\omega t - bx - \phi]. \quad (3)$$

Here the angular frequency  $\omega = 2\pi/\tau$ , where  $\tau$  denotes the period of oscillations of the temperature. In practice, it is of the order of 12 minutes (the heater works 6 min. then it is off during next 6 min. and so on). Similarly,  $b = 2\pi/\Lambda$ , where  $\Lambda$  is the spatial period of the wave. It may be shown that constants  $a$  and  $b$  are coupled to  $\lambda$  in the following way:

$$\lambda = \rho c \frac{\omega}{2ab}, \quad (4)$$

where  $\rho$  denotes the density of the material,  $c$  – its specific heat. The factor  $(T_0 e^{-ax})$  has the meaning of the amplitude of oscillations at the point  $x$ .

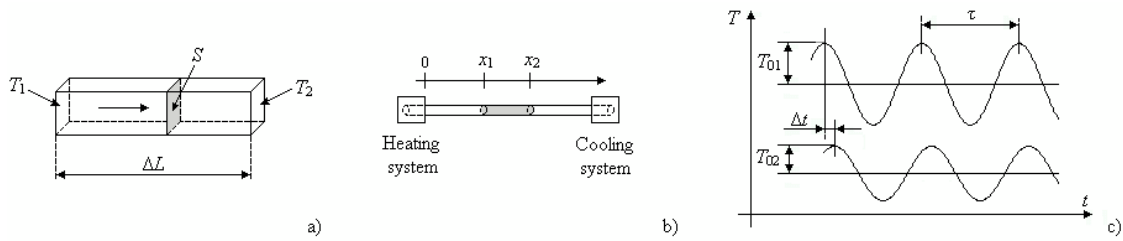


Fig. 6

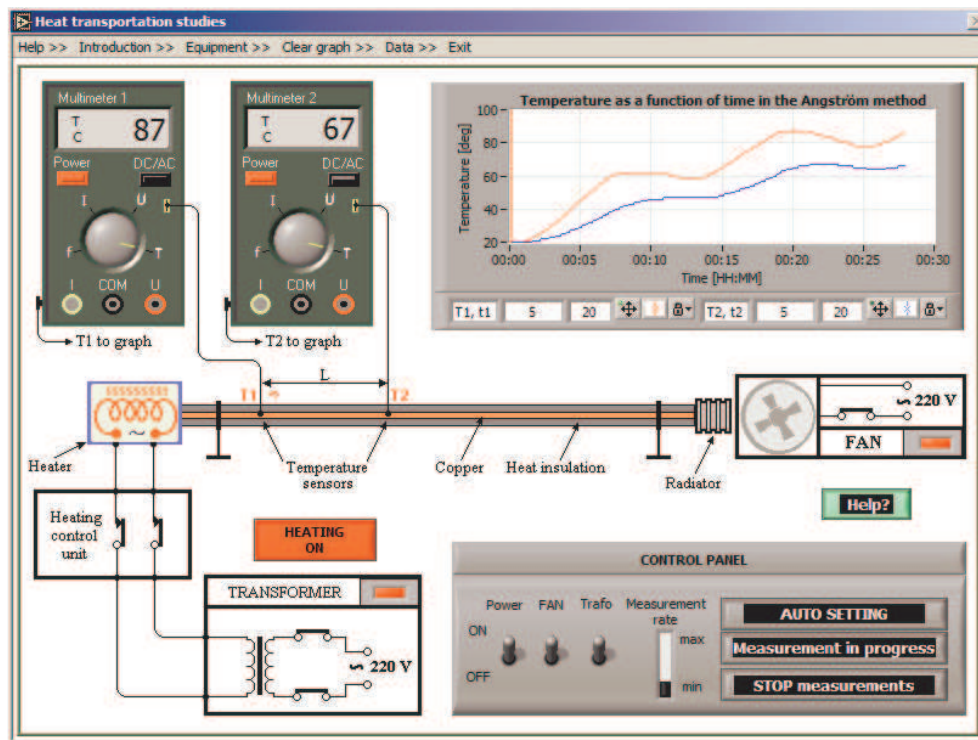


Fig. 7

By measuring the amplitudes  $T_{01}$  and  $T_{02}$  (Fig. 6c) in two points  $x_1$  and  $x_2$ , separated by a distance  $\Delta L$  (Fig. 6b), one can easily calculate the thermal conductivity coefficient  $\lambda$ . It is equal to

$$\lambda = \frac{\rho c (\Delta L)^2}{2 \Delta t \ln(T_{01}/T_{02})} \quad (5)$$

where  $\Delta t$  denotes the temporal phase shift between oscillations in both points.

The front panel of the virtual experimental set-up of the simulated experiment used for measurement of heat conductivity based on Angström method is shown in Fig. 7.

### Electrical resonance studies

Resonance phenomenon is demonstrated, on examples of electrical resonance circuits, both parallel and serial version. The front panel of the virtual experimental set-up of simulated experiment used for electrical resonance studies is shown in Fig. 8.

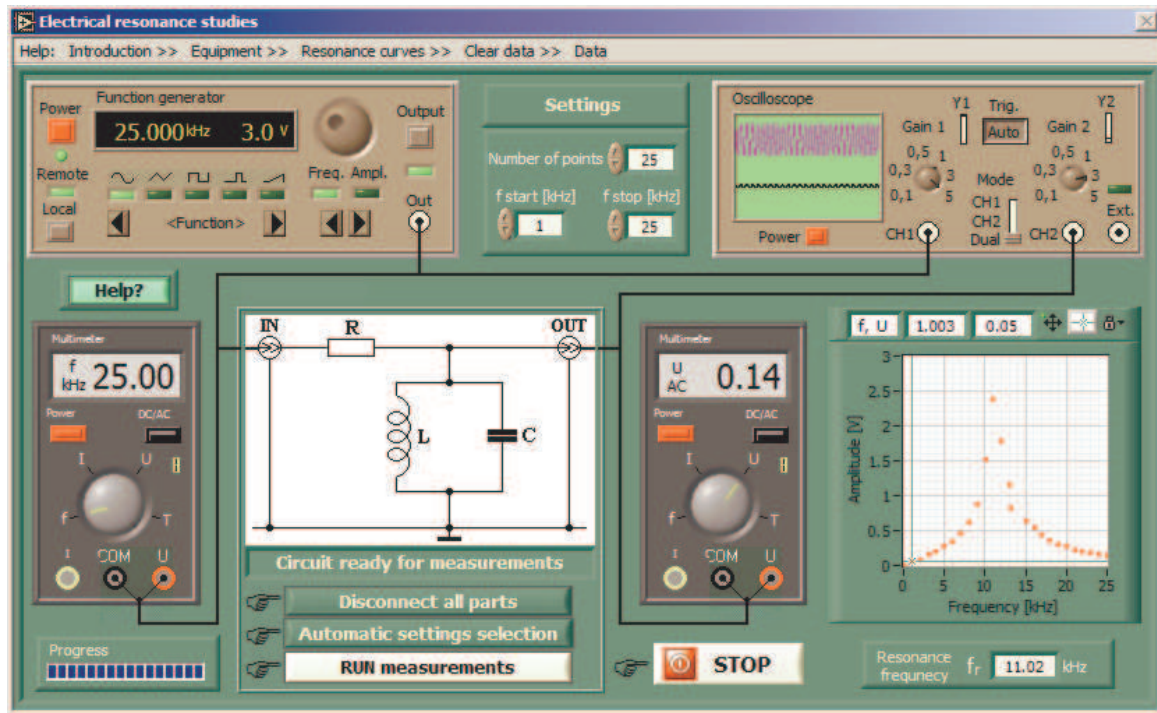


Fig. 8

The current and voltage as a function of the frequency can be observed in the parallel and series tuned  $LC$  circuits. Dependence circuit configuration, selected on the front panel, one can observe a voltage or a current resonance.

*Voltage resonance – serial resonance.*  $RLC$  serial resonance circuit is shown in Fig. 9a. In this configuration  $L$  denotes an inductance of the inductor,  $C$  a capacitance of the capacitor,  $r_L$  and  $r_C$  loss resistance of the inductor and the capacitor respectively,  $R_d$  a damping resistance,  $R_S$  a source resistance and  $e(t)$  an alternating voltage source. The equivalent circuit diagram is shown in Fig. 9b. The relation between  $e(t)$  and  $i(t)$  is given by



$$e(t) = i(t)R + L \frac{di(t)}{dt} + \frac{Q_C}{C} \quad (6)$$

where  $e(t) = E_m \cos(\omega t)$ ;  $i(t)$  is the current;  $Q_C$  is the charge of the capacitor;  $R = R_S + R_d + r_L + r_C$ .

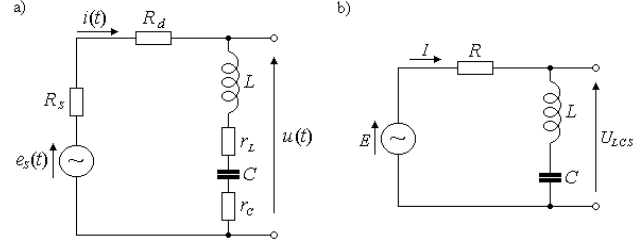


Fig. 9

If equation (6) is differentiated and solved for  $i$ , one obtains:

$$i(t) = I_m \cos(\omega t - \varphi_s) = \frac{E_m}{|Z|} \cos(\omega t - \varphi_s), \quad (7)$$

where  $\omega = 2\pi f$ .

The absolute value of the total impedance  $|Z|$  is given by

$$|Z| = \frac{E_m}{I_m} = \sqrt{R^2 + \left( \omega L - \frac{1}{\omega C} \right)^2}, \quad (8)$$

and the phase displacement  $\varphi_s$  between the current and the voltage is given by

$$\varphi_s = -\arctan \left( \frac{\omega L - \frac{1}{\omega C}}{R} \right). \quad (9)$$

At the resonance point  $\omega L = 1/\omega C$ , and the resonance frequency  $f_r$  is given by

$$f_r = 1/(2\pi\sqrt{LC}). \quad (10)$$

The relationship between the quality factor  $Q_s$  and bandwidth  $B$  is given by

$$B = (f_2 - f_1) = f_r / Q_s, \quad (11)$$

where  $f_1$  and  $f_2$  are frequencies, at which  $I_1/I_r = I_2/I_r = 1/\sqrt{2}$ ,  $I_r$  is the current  $I$  at resonance frequency and

$$Q_s = \omega_r L / R = 1/(\omega_r C R). \quad (12)$$

*Current resonance – parallel resonance.* Figure 10a shows  $RLC$  parallel resonance circuit. The equivalent circuit diagram is shown in Fig. 10b. In this configuration  $R_d$  denotes a dynamic resistance and the resistance  $R$  consists of the resistance  $R_s$  added to the resistance  $R_{LEAD}$ . Therefore  $R = R_s + R_{LEAD}$ .

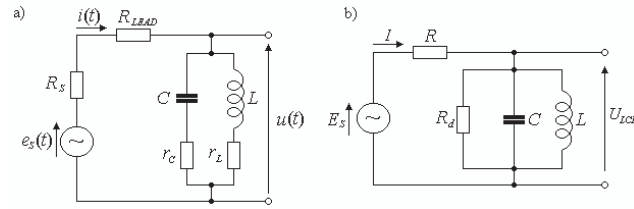


Fig. 10

The absolute value of the total  $LCR_d$  admittance  $|Y|$  is given by

$$|Y| = \frac{I_m}{E_m} = \sqrt{(G)^2 + \left( \omega C - \frac{1}{\omega L} \right)^2}, \quad (13)$$

where  $G = 1/R_d$ .

The phase displacement  $\varphi_P$  between the current and the voltage is given by

$$\varphi_P = -\arctan \left( \frac{\omega C - \frac{1}{\omega L}}{G} \right), \quad (14)$$

Parallel resonance occurs if  $\omega = \omega_r = 1/\sqrt{LC}$ .

## Laws of gases

It is a set of simulated experiments demonstrating the basic thermodynamic processes for ideal gas. In opposite to the rest of experiments described previous, here emphasis is placed on mathematical model rather than on measurement. It is because the experiment is addressed

mainly for schools and it was developed as a model example of a simple simulated experiment developed in LabVIEW.

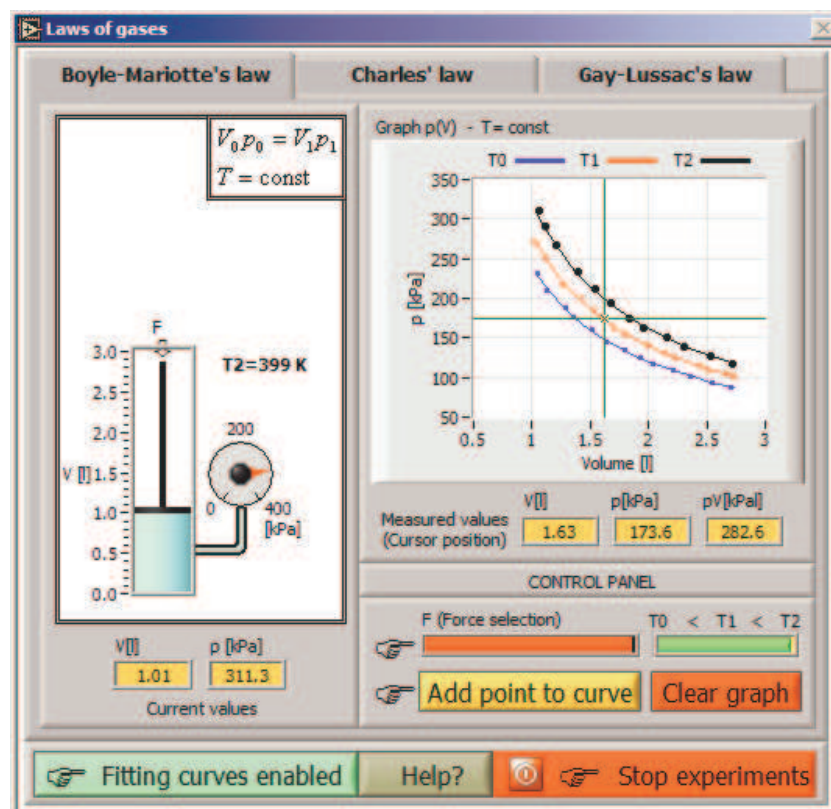


Fig. 11

The front panel of the set of the virtual experimental set-up used for Boyle-Mariotte's, Charles's and Gay-Lussac's laws presentation is shown in Fig. 11.

### Conclusions

In the paper a set of virtual physics experiment was described with highlight on their special features. The presented set of eight simulated physics experiments are included in a specific module for training, dedicated for the in-service teachers training, in the frame of a recent approved European Socrates project: 128989-CP-1-2006-1-RO-COMENIUS-C21. The training module consists of 6 face-to-face meetings and provides both technical and pedagogical elements with the view of the implementation in the classroom of the proposed virtual applications. The content of the units is oriented on: basics of virtual instrumentation, teaching methodologies and pedagogical strategies involved in the using of the virtual instrumentation, virtual instruments and specific programming languages, basic steps in developing a virtual instrument, virtual instrumentation application designing and implementing.

### Bibliography

- [1]. Socrates Programme, ANPS, Warsaw 2004.
- [2]. Tłaczała W.: *Virtual Instrumentation in Physics*. Handbook of Measuring System Design edited by Peter Sydenham and Richard Thorn. © John Wiley & Sons Ltd (2005) pp. 695-701.
- [3]. Tłaczała W., Gorghiu G., Glava A. E., Bazan P., Kukkonen J., Maśior W., Użycki J., and Zaremba M., *Computer simulation and modeling in virtual physics experiments*,

Proceedings of IV International Conference on Multimedia and Information & Communication Technologies in Education. November 22-25<sup>th</sup> 2006, Seville, Spain.